

Chemistry of C-Trimethylsilyl-Substituted Heterocarboranes. 29. Synthetic and Structural Studies on Lanthanacarboranes with Two and Three “Carbons Apart” Carborane Cages Bonding to Ln(III) Metal (Ln(III) = Nd, Gd, Dy, Ho, Er, Tb, Lu)

Jianhui Wang,^{†,‡} Shoujian Li,[†] Chong Zheng,[†] John A. Maguire,[‡] Biprajit Sarkar,[§] Wolfgang Kaim,[§] and Narayan S. Hosmane*,^{†,§}

Department of Chemistry and Biochemistry, Northern Illinois University, DeKalb, Illinois 60115-2862, Department of Chemistry, Southern Methodist University, Dallas, Texas 75275-0314, and Institut für Anorganische Chemie, Universität Stuttgart, Pfaffenwaldring 55, Stuttgart D-70550, Germany

Received June 3, 2003

The reactions of *closo-exo*-5,6-Na(THF)₂-1-Na(THF)₂-2,4-(SiMe₃)₂-2,4-C₂B₄H₄ (**1**) with anhydrous LnCl₃ (Ln = Nd, Gd, Dy, Ho, Er, Tb, Lu), in molar ratios of 2:1 in dry benzene (C₆H₆) at 60 °C, produced the full-sandwich lanthanacarborane complexes 2,2',4,4'-(SiMe₃)₄-3,5',6'-[(μ-H)₃Na(X)_n(Y)_m]-1,1'-*commo*-Ln(η⁵-2,4-C₂B₄H₄)₂ (**2**, Ln = Nd, X = THF, n = 2, Y = none; **3**, Ln = Gd, X = THF, n = 3, Y = none; **4**, Ln = Dy, X = THF, n = 1, Y = TMEDA, m = 1; **5**, Ln = Ho, X = DME, n = 1, Y = none; **6**, Ln = Er, X = THF, n = 1; Y = none; **7**, Ln = Tb, X and Y = none; **8**, Ln = Lu, X = THF, n = 2) in 70–93% yields. However, the reactions of **1** at 60 °C with anhydrous LnCl₃ (Ln = Dy, Er), at carborane to Ln molar ratios of 3:1 in dry benzene (C₆H₆), gave novel metallocarboranes, analogues of Cp₃Ln, with the formula [Na₃][1,1'-[5,6-(μ-H)₂-*nido*-2,4-(SiMe₃)₂-2,4-C₂B₄H₄]-2,2',4,4'-(SiMe₃)₄-1,1'-*commo*-Ln-(2,4-C₂B₄H₄)₂] (**9**, Ln = Dy; **10**, Ln = Er) as yellow crystalline solids in 78 and 82% yields, respectively. While compounds **2–5** and **8–10** were characterized by single-crystal X-ray diffraction studies, the diamagnetic compound **8** was also characterized by ¹H, ¹³C, and ¹¹B NMR spectroscopy and compounds **2**, **3**, and **5** were studied by EPR spectroscopy. Compounds **2**, **4**, and **8** were found to be isostructural with bent-sandwich geometries, in which a Ln(III) center is coordinated to two carborane ligands. The solvated Na⁺ ions, present in each molecule for charge compensation, do not seem to influence the cage geometries. Complexes **2**, **4**, and **8** crystallized in the triclinic space group *P* $\bar{1}$, complexes **3**, **9**, and **10** were found to crystallize in the monoclinic space group *P*2₁/*n*, and complex **5** crystallized in the monoclinic space group *C*2/*c*. The final refinements of **2–5** and **8–10** converged at R1 = 0.0223, 0.0664, 0.0418, 0.0557, 0.0639, 0.0596, and 0.0770 and at wR2 = 0.0593, 0.1265, 0.1125, 0.1457, 0.1413, 0.1225, and 0.1594, respectively. The room-temperature magnetic susceptibilities of **9** and **10** were found to be 10.4 and 9.76 μ_B per metal atom, respectively.

Introduction

The first report of the synthesis and structural characterization of an f-block metallocarborane was that of the uranacarborane [U(C₂B₉H₁₁)₂Cl₂]²⁻ in 1977,¹ followed in 1988 by reports for the compounds *closo*-3-Yb(DMF)₄-1,2-C₂B₉H₁₁ and [3,3'-(THF)₂-*commo*-3,3'-Sm-(C₂B₉H₁₁)₂]⁻².² Since these initial reports, a number of lanthanide complexes, mainly with the C₂B₁₀ and C₂B₉ cage systems, have been described.³ Our interest has been directed at lanthanide complexes of the C₂B₄ cage

systems,⁴ which exhibit reaction characteristics that are not found in the larger cages. For example, reactions of the THF-solvated dilithium salt of the [2,3-(SiMe₃)₂C₂B₄H₄]²⁻ dianion with anhydrous LnCl₃ in a molar ratio of 2:1 in dry benzene and THF produced trinuclear Ln(III) carboranes of the form {[η⁵-1-Ln-2,3-(SiMe₃)₂-2,3-C₂B₄H₄]₃[(μ₂-1-Li-2,3-(SiMe₃)₂-2,3-C₂B₄H₄]₃-(μ₃-OMe)][(μ₂-Li(THF))₃(μ₃-O)]} (Ln = Sm, Gd, Tb, Dy, Ho, Nd), instead of the expected full-sandwich lanthanacarboranes.^{4a,d,g,k} These clusters are composed of three half-sandwich lanthanacarboranes and three lithiacarboranes arranged around an oxide ion and a methoxide ion, respectively.^{4g} These unusual products were believed to arise from the initial formation of a half-sandwich lanthanacarborane, which reacts further with

* To whom correspondence should be addressed at Northern Illinois University. E-mail: nhosmane@niu.edu.

[†] Northern Illinois University.

[‡] Southern Methodist University.

[§] Universität Stuttgart.

(1) Fronczek, F. R.; Halstead, G. W.; Raymond, K. N. *J. Am. Chem. Soc.* **1977**, *99*, 1769–1775.

(2) Manning, M. J.; Knobler, C. B.; Hawthorne, M. F. *J. Am. Chem. Soc.* **1988**, *110*, 4458–4459.

(3) For recently reviews see: (a) Saxena, A. K.; Hosmane, N. S. *Chem. Rev.* **1993**, *93*, 1081–1124. (b) Xie, Z. *Coord. Chem. Rev.* **2002**, *231*, 23–46.

the THF solvent, or its decomposition product, to form the final trinuclear cluster. On the other hand, the reaction of the TMEDA-solvated dilithium salt of the [2,3-(SiMe₃)₂C₂B₄H₄]²⁻ dianion with anhydrous LnCl₃ at a 2:1 molar ratio produced the full-sandwich species [1-Cl-1-(μ-Cl)-2,2',3,3'-(SiMe₃)₄-5,6-[(μ-H)₂Li(TMEDA)]-4,4',5,5'-[(μ-H₃)Li(TMEDA)-*commo*-Ln(2,3-C₂B₄H₄)₂]⁻ (Ln = Sm, Gd, Dy, Ho, Er).^{4e,h} In addition, several half-sandwich complexes have been reported.^{4j,l} These results show that, in addition to the molar ratios of the carborane ligand and LnCl₃ reactants, the nature of the solvent plays an important role in determining the products of the f-block metalation reactions of the C₂B₄ cages. Since most of the metalation reactions were run using either a 1:1 or 2:1 carborane to LnCl₃ molar ratio, the consequences of using higher reaction ratios have not been investigated. This would be of interest, since LnCp₃ complexes in which the three Cp⁻ ligands are η⁵ bonded to a lanthanide metal have been reported.⁵ Most of the small-cage lanthanocarboranes have involved the use of the so-called "carbons adjacent" (2,3-C₂B₄) isomer, in which the two cage carbons occupy adjacent positions in the C₂B₃ open face of the carborane. There is also a "carbons apart" (2,4-C₂B₄) isomer in which the two carbon atoms on the face are separated by a boron atom; these also form metallacarboranes.^{3a,6} Although both full- and half-sandwich complexes have been reported,⁷ the lanthanocarboranes in "carbons apart" cage systems have not been studied systematically. Herein we present a full report on the syntheses and crystal structures of a number of "carbons apart" lanthanocarborane complexes, some of which have been recently described in preliminary communications.^{7b,c}

Experimental Section

Materials. Benzene, *N,N,N,N*-tetramethylethylenediamine (TMEDA), ethylene glycol, dimethyl ether (DME),

(4) (a) Oki, A. R.; Zhang, H.; Hosmane, N. S. *Angew. Chem., Int. Ed. Engl.* **1992**, *31*, 432–434. (b) Hosmane, N. S.; Maguire, J. A. *J. Cluster Sci.* **1993**, *4*, 297–349. (c) Hosmane, N. S.; Wang, Y.; Oki, A. R.; Zhang, H.; Zhu, D.; McDonald, E. M.; Maguire, J. A. *Phosphorus, Sulfur, Silicon Relat. Elem.* **1994**, *93–94*, 253–256. (d) Zhang, H.; Oki, A. R.; Wang, Y.; Maguire, J. A.; Hosmane, N. S. *Acta Crystallogr., Sect. C: Cryst. Struct. Commun.* **1995**, *C51*, 635–638. (e) Hosmane, N. S.; Wang, Y.; Zhang, H.; Oki, A. R.; Maguire, J. A.; Waldhör, E.; Kaim, W.; Binder, H.; Kremer, R. K. *Organometallics* **1995**, *14*, 1101–1103. (f) Zhang, H.; Wang, Y.; Maguire, J. A.; Hosmane, N. S. *Acta Crystallogr., Sect. C: Cryst. Struct. Commun.* **1996**, *C52*, 8–11. (g) Hosmane, N. S.; Wang, Y.; Oki, A. R.; Zhang, H.; Maguire, J. A. *Organometallics* **1996**, *15*, 626–638. (h) Hosmane, N. S.; Wang, Y.; Zhang, H.; Maguire, J. A.; McInnis, M.; Gray, T. G.; Collins, J. D.; Kremer, R. K.; Binder, F. H.; Waldhör, E.; Kaim, W. *Organometallics* **1996**, *15*, 1006–1013. (i) Zhang, H.; Wang, Y.; Maguire, J. A.; Hosmane, N. S. *Acta Crystallogr., Sect. C: Cryst. Struct. Commun.* **1996**, *C52*, 640–643. (j) Hosmane, N. S.; Oki, A. R.; Zhang, H. *Inorg. Chem. Commun.* **1998**, *1*, 101–104. (k) Zheng, C.; Hosmane, N. S.; Zhang, H.; Zhu, D.; Maguire, J. A. *Internet J. Chem.* **1999**, *2*, 10 (URL: <http://www.ijc.com/articles/1999v2/10/>). (l) Hosmane, N. S.; Wang, Y.; Zhang, H.; Zhu, Y.; Maguire, J. A. *Inorg. Chem. Commun.* **2001**, *4*, 547–550.

(5) Edelmann, F. T. In *Comprehensive Organometallic Chemistry II*; Abel, E. W., Stone, F. G. A., Wilkinson, G., Eds.; Pergamon Press: Oxford, U.K., 1995; Vol. 4, Chapter 2, pp 11–212.

(6) (a) Hosmane, N. S.; Zhang, H.; Jia, L.; Colacot, T. J.; Maguire, J. A.; Wang, X.; Hosmane, S. N.; Brooks, K. A. *Organometallics* **1999**, *18*, 516. (b) Hosmane, N. S.; Zhu, D.; Zhang, H.; Oki, A. R.; Maguire, J. A. *Organometallics* **1998**, *17*, 3196.

(7) (a) Hosmane, N. S.; Li, S.-J.; Zheng, C.; Maguire, J. A. *Inorg. Chem. Commun.* **2001**, *4*, 104–107. (b) Wang, J.; Li, S.; Zheng, C.; Maguire, J. A.; Hosmane, N. S. *Organometallics* **2002**, *21*, 3314–3316. (c) Wang, J.; Li, S.; Zheng, C.; Maguire, J. A.; Hosmane, N. S. *Organometallics* **2002**, *21*, 5149–5151. (d) Wang, J.; Li, S.; Zheng, C.; Maguire, J. A.; Hosmane, N. S. *Inorg. Chem. Commun.* **2002**, *5*, 602–605.

Table 1. Preparation and Selected Physical Properties of 2–10

compd	LnCl ₃	amt of LnCl ₃ (g, mmol)	amt of carborane ligand ^a (g, mmol)	color	mp (°C)	yield ^b (g, mmol, %)
2	NdCl ₃	0.38, 1.52	1.70, 3.08	green	>250	1.00, 1.34, 88
3	GdCl ₃	0.40, 1.52	1.70, 3.08	yellow	175 dec	1.08, 1.30, 86
4	DyCl ₃	0.43, 1.60	1.77, 3.21	yellow	>250	0.96, 1.13, 70
5	HoCl ₃	0.43, 1.59	1.77, 3.21	pink	>250	1.00, 1.40, 88
6	ErCl ₃	0.18, 0.66	0.71, 1.28	orange	>240	0.37, 0.50, 76
7	TbCl ₃	0.17, 0.64	0.71, 1.28	colorless	>250	0.37, 0.60, 93
8	LuCl ₃	0.43, 1.53	1.76, 3.19	colorless	>240	1.14, 1.35, 88
9	ErCl ₃	0.29, 1.06	1.76, 3.19	pink	>250	0.84, 0.87, 82
10	DyCl ₃	0.28, 1.04	1.76, 3.19	yellow	>250	0.80, 0.83, 78

^a *closo-exo*-5,6-Na(THF)₂-1-Na(THF)₂-2,4-(SiMe₃)₂-2,4-C₂B₄H₄.

^b Yield is based on LnCl₃ consumed.

tetrahydrofuran (THF), and *n*-hexane were dried over NaH or Na/benzophenone and doubly distilled before use. All other solvents were dried over 4–8 Å mesh molecular sieves (Aldrich) and were either saturated with dry argon or degassed before use. The synthesis of *closo-exo*-5,6-Na(THF)₂-1-Na(THF)₂-2,4-(SiMe₃)₂-2,4-C₂B₄H₄ followed the published procedure.⁸ Prior to use, NdCl₃, GdCl₃, TbCl₃, DyCl₃, HoCl₃, ErCl₃, and LuCl₃ (Aldrich) were degassed in vacuo at 130 °C for 24 h.

Spectroscopic and Analytical Procedures. Proton, boron-11, and carbon-13 NMR spectra were recorded on a Bruker Fourier transform multinuclear NMR spectrometer at 200, 64.2, and 50.3 MHz, respectively. Infrared spectra were recorded on a Perkin-Elmer Model 1600 FT-IR spectrophotometer and Nicolet Magna 550 FT-IR spectrophotometer. EPR spectra were recorded on a Bruker ESP 300 spectrometer equipped with an ER035 gaussmeter (Bruker), a 5350B microwave counter (HP), and an ESR 900 continuous flow cryostat (Oxford Instruments).

Elemental analyses were determined in house at Northern Illinois University using a Perkin-Elmer 2400 CHN elemental analyzer.

Magnetic Susceptibility. Magnetic susceptibilities were measured with a MPMS Quantum Design SQUID magnetometer between 5 K and room temperature in a magnetic field of 1 T. The samples (~20 mg) were contained in gelatin capsules,⁹ the magnetizations of which were determined in separate runs and subtracted. Corrections for core diamagnetism were not applied.

Synthetic Procedures. All experiments were carried out in 100 mL Pyrex glass round-bottom flasks, equipped with magnetic stirring bars and high-vacuum Teflon valves. After their initial purifications, nonvolatile substances were manipulated in either a drybox or a glovebag under an atmosphere of dry nitrogen. All known compounds among the products were identified by comparing their IR and/or ¹H NMR spectra with those of authentic samples.

Synthesis of 2,2',4,4'-(SiMe₃)₄-3,5',6'-[(μ-H)₃Na(X)_n(Y)_m]-1,1'-*commo*-Ln(η⁵-2,4-C₂B₄H₄)₂ (2, Ln = Nd, X = THF, *n* = 2, Y = none; 3, Ln = Gd, X = THF, *n* = 3, Y = none; 4, Ln = Dy, X = THF, *n* = 1, Y = TMEDA, *m* = 1; 5, Ln = Ho, X = DME, *n* = 1, Y = none; 6, Ln = Er, X = THF, *n* = 1, Y = none; 7, Ln = Tb, X, Y = none; 8, Ln = Lu, X = THF, *n* = 2; Y = none). Except for the quantities used, the procedures in the syntheses of compounds 2–8 were identical. Therefore, only one typical synthesis will be described; the details of quantities used, product yields, and certain physical properties of 2–8 are summarized in Table 1.

A previously weighed sample of *closo-exo*-5,6-Na(THF)₂-1-Na(THF)₂-2,4-(SiMe₃)₂-2,4-C₂B₄H₄ (**1**) was mixed with anhydrous LnCl₃ in a molar ratio of 2:1, in about 20–30 mL of dry

(8) Hosmane, N. S.; Jia, L.; Zhang, H.; Bausch, J. W.; Prakash, G. K. S.; Williams, R. E.; Onak, T. P. *Inorg. Chem.* **1991**, *30*, 3793–3795.

(9) Commercially available pharmaceutical gelatin capsules.

Table 2. Infrared Absorptions (cm⁻¹, KBr Pellet)^a

compd	absorption
2	2950 (vs), 2888 (m), 2570 (m), 2520(m), 2462 (m), 2423 (m), 2270 (m), 1394 (vs), 1337 (br), 1241 (vs), 1171 (m), 1049 (m), 1025 (w), 835 (vs), 760 (m), 679 (m), 625 (m)
3	2952 (vs), 2892 (m), 2562(m), 2510 (m), 2468 (m), 2373 (m), 1399 (vs), 1306 (br), 1243 (vs), 1176 (m), 1048 (m), 836 (vs), 757 (m), 685 (m), 631 (m)
4	2953 (vs), 2889 (m), 2830 (m), 2789 (m), 2518 (m), 2475 (m), 2441 (m), 2357 (m), 1455 (m), 1399 (s), 1289 (w), 1238 (vs), 1171 (s), 1095 (m), 1018 (m), 944 (m), 835 (vs), 756 (m), 684 (m), 629 (m)
5	2953 (vs), 2893 (m), 2855 (m), 2537 (s), 2509 (s), 2462 (s), 1458 (m), 1400 (s), 1240 (vs), 1177 (s), 1137 (m), 1073 (m), 1019 (s), 948 (m), 926 (w), 837 (vs), 760 (s), 684 (m), 632 (m)
6	2952 (vs), 2894 (m), 2573 (m), 2498 (m), 2436 (m), 2379 (m), 1378 (m), 1240 (vs), 1168 (s), 1112 (w), 1051 (m), 837 (vs), 748 (s), 680 (m), 628 (m)
7	2955 (vs), 2592 (w), 2520 (br), 1409 (br), 1255 (vs), 1193 (w), 1091 (s), 1015 (s), 815 (vs), 676 (m), 625 (m)
8	2953 (vs), 2893 (m), 2573 (m), 2529 (m), 2479 (m), 2383 (m), 1398 (m), 313 (w), 1243 (vs), 1176 (s), 1048 (m), 934 (w), 834 (vs), 757 (s), 680 (m), 629 (m)
9	2956 (vs), 2895 (m), 2506 (s), 2467 (br), 2432 (br), 2360 (s), 2283 (s), 1383 (br), 1254 (vs), 1084 (vs), 1016 (vs), 833 (vs), 803 (vs), 681 (m)
10	2947 (vs), 2891 (m), 2512 (s), 2468 (br), 2434 (br), 2353 (s), 2282 (s), 2236 (s), 1596 (br), 1381 (m), 1241 (vs), 1176 (br), 1099 (m), 1059 (m), 1031 (w), 835 (vs), 750 (m), 685 (s), 626 (m)

^a Legend: v = very, s = strong or sharp, m = medium, w = weak, sh = shoulder, br = broad.

benzene and stirred at 0 °C for 2–3 h. The reaction mixture was warmed to room temperature, raised to 60 °C, and then stirred for an additional 24 h. During this period the solution became turbid and turned the color of the particular complex that is listed in Table 1. The heterogeneous product mixture was filtered through a frit, and the residue was washed repeatedly with anhydrous benzene. The solid that remained on the frit after the washings was identified by qualitative analysis as NaCl (not measured) and was discarded. Removal of solvents from the clear solution gave a solid that was later recrystallized from different solvent mixtures (*n*-hexane/benzene (10/90 v/v) for **2**, **3**, and **6–8**; TMEDA/THF/*n*-hexane (1:2:7 v/v/v) for **4**; DME/hexanes (40:60 v/v) for **5**) to collect air-sensitive crystals, identified as a dimer of 2,2',4,4'-(SiMe₃)₄-3,5',6'-[(μ-H)₃Na(X)_n(Y)_m]-1,1'-*commo*-Ln(η⁵-2,4-C₂B₄H₄)₂ (**2**, Ln = Nd, X = THF, *n* = 2, *m* = 0; **3**, Ln = Gd, X = THF, *n* = 3, *m* = 0; **4**, Ln = Dy, X = THF, *n* = 1, Y = TMEDA, *m* = 1; **5**, Ln = Ho, X = DME, *n* = 1, *m* = 0; **6**, Ln = Er, X = THF, *n* = 1.5, *m* = 0; **7**, Ln = Tb, *n*, *m* = 0; **8**, Ln = Lu, X = THF, *n* = 2, *m* = 0). Anal. Calcd (found) for (C₁₆H₄₄B₈Si₄NaNd)·2THF (**2**): C, 38.60 (38.54); H, 8.10 (8.15). Calcd (found) for (C₁₆H₄₄B₈-Si₄NaGd)·3THF (**3**): C, 40.43 (40.66); H, 8.24 (8.35). Calcd (found) for [(C₁₆H₄₄B₈Si₄NaDy)·(TMEDA)·THF]·C₆H₆ (**4**): C, 41.07 (41.16); H, 8.44 (8.25); N, 3.30 (3.60). Calcd (found) for (C₁₆H₄₄B₈Si₄NaHo)·DME (**5**): C, 34.25 (34.16); H, 7.76 (7.74). Calcd (found) for (C₁₆H₄₄B₈Si₄NaEr)·2·3THF (**6**): C, 36.01 (36.21); H, 7.69 (7.78). Calcd (found) for C₁₆H₄₄B₈Si₄NaTb (**7**): C, 31.13 (31.41); H, 7.19 (7.40). Calcd (found) for (C₁₆H₄₄B₈-Si₄NaLu)·3THF (**8**): C, 39.57 (39.92); H, 8.07 (7.92). The infrared spectral data, with selected assignments for **2–8**, are presented in Table 2. NMR data for complex **8**: ¹H NMR (C₆D₆, relative to external Me₄Si) δ 3.71 (s (br), 2 H, THF), 1.56 (s (br), 2 H, THF), 0.74 (s, 3 H, SiMe₃), 0.68 (s, 3 H, SiMe₃); ¹³C NMR (C₆D₆, relative to external Me₄Si) δ 128.6 (s (br), cage carbons (SiCB)), 70.6 (m, THF), 24.9 (m, THF), 2.19 (q (br), SiMe₃), 1.84 (q (br), SiMe₃, ¹J(¹³C–¹H) = 118.5 Hz); ¹¹B NMR (THF, external BF₃·OEt₂) δ 28.5 (br, 1B, basal BH), 7.0 (br, 2B, basal BH), -47.3 (d, 1B, apical BH), ¹J(¹¹B–¹H) = 161 Hz).

Synthesis of [Na₃][1,1'-{5,6-(μ-H)₂-*nido*-2,4-(SiMe₃)₂-2,4-C₂B₄H₄}-2,2',4,4'-(SiMe₃)₄-1,1'-*commo*-Ln-(2,4-C₂B₄H₄)₂] (9**, Ln = Dy; **10**, Ln = Er).** A previously weighed sample of *closo*-exo-5,6-Na(THF)₂-1-Na(THF)₂-2,4-(SiMe₃)₂-2,4-C₂B₄H₄ (**1**) was mixed with anhydrous LnCl₃, in a molar ratio of 3:1, in dry benzene (about 10–15 mL) and stirred at 60 °C for 24 h, during which time the solution turned yellow and became turbid. The heterogeneous product mixture was then filtered, in vacuo, and the solvent removed from the filtrate to collect a pale yellow solid. The particular solid was extracted in benzene and then filtered again to collect a clear yellow solution. Removal of the solvent from this solution gave a yellow solid that was later recrystallized from dry *n*-hexane to collect air-sensitive crys-

tals, identified as [Na₃][1,1'-{5,6-(μ-H)₂-*nido*-2,4-(SiMe₃)₂-2,4-C₂B₄H₄}-2,2',4,4'-(SiMe₃)₄-1,1'-*commo*-Ln-(2,4-C₂B₄H₄)₂] (**9**, Ln = Dy; **10**, Ln = Er). Anal. Calcd (found) for [C₂₄H₆₆B₁₂Si₆Na₃Dy·(C₆H₆)]₃·2C₆H₁₄ (**9**): C, 40.04 (40.37); H, 8.03 (7.80). Anal. Calcd (found) for C₂₄H₆₆B₁₂Si₆Na₃Er·C₆H₆ (**10**): C, 37.25 (37.78); H, 7.50 (7.68). The yields are shown in Table 1, and the infrared spectral data for **9** and **10** are given in Table 2.

X-ray Analyses of 2–5 and 8–10. X-ray-quality crystals of **2**, **3**, and **8–10** were grown from an *n*-hexane/benzene (10/90 v/v) solution by slow evaporation. Good-quality crystals of **4** were obtained from a TMEDA/THF/*n*-hexane (1:2:7 v/v/v) mixture, while crystals of the holmacarborane **5** were grown from a DME/hexanes (40/60 v/v) solution. The crystals were mounted on a Bruker SMART CCD PLATFORM diffractometer, under a low-temperature nitrogen stream. The pertinent crystallographic data for **2–5** and **8–10** are summarized in Tables 3 and 4, respectively. Compounds **2**, **4**, and **8** were found to be isostructural, whose space groups were uniquely determined from systematic absences as *P1*. Similar measurements on **3** were consistent with the space group *P2*₁/*n*, while **5** was found to be in the *C2/c* space group. Compounds **9** and **10** were also found to be isostructural, and their space groups were uniquely determined as *P2*₁/*n*. Intensity data for compounds **2–5** and **8–10** were collected at 173 K. All data considered as observed (*I* > 2σ(*I*)) were corrected for Lorentz, polarization, and absorption effects (G. M. Sheldrick, SADABS, Program for Empirical Absorption Correction of Area Detector Data, University of Göttingen, Göttingen, Germany, 1996). Semiempirical absorption studies (SADABS) were applied for each structure, and the relevant minimum and maximum transmission factors are listed in Tables 3 and 4. All structures were solved by direct methods and refined by full-matrix least-squares techniques using the SHELXTL system of programs.¹⁰ All structures were refined on *F*² for all reflections.¹¹ Weighted wR2 and goodness of fit values were based on *F*². For **9** and **10**, nonsolvating benzene molecules and *n*-hexanes were present in each structure, while only nonsolvating benzene was present in **4**. In structure **4**, the geometrical centroid of the benzene molecule was located at the interval of the structure. In structure **9** and **10**, the benzene and *n*-hexane possessed the interval between the two sodium cations from the two neighboring units. Full-matrix refinement was performed for each structure. In all of the structures, the non-H atoms were refined anisotropically. The carborane-cage H atoms of **2–5** were located in difference Fourier maps. The final values of R1 and weighted wR2 are listed in Tables 3 and 4. The selected interatomic distances and angles are listed in Tables 5 and 6,

(10) Sheldrick, G. M. SHELXTL, Version 5.1; Bruker Analytical X-ray Systems, Madison, WI, 1997.

(11) Sheldrick, G. M. SHELXL93; Program for the Refinement of Crystal Structures; University of Göttingen, Germany, 1993.

Table 3. Crystallographic Data^a for Complexes 2–5 and 8

	2	3	4	5	8
formula	C ₂₄ H ₆₀ B ₈ N-NdO ₂ Si ₄	C ₂₈ H ₆₈ B ₈ N-GdO ₃ Si ₄	C ₂₉ H ₇₁ B ₈ N-DyN ₂ O ₂ Si ₄	C ₂₀ H ₅₄ B ₈ N-HoO ₂ Si ₄	C ₂₄ H ₆₀ B ₈ N-LuO ₂ Si ₄
fw	746.79	831.90	848.21	713.39	777.52
cryst syst	triclinic	monoclinic	triclinic	monoclinic	triclinic
space group	<i>P</i> $\bar{1}$	<i>P</i> ₂ / <i>n</i>	<i>P</i> $\bar{1}$	<i>C</i> 2/ <i>c</i>	<i>P</i> $\bar{1}$
<i>a</i> , Å	11.317(2)	11.644(2)	12.258(4)	21.334(5)	13.933(3)
<i>b</i> , Å	12.648(2)	17.426(3)	13.734(4)	13.359(3)	17.236(4)
<i>c</i> , Å	15.159(3)	22.031(4)	15.028(5)	27.138(6)	17.828(4)
α , deg	102.501(3)	90	93.647(5)	90	92.569(4)
β , deg	92.293(3)	92.244(4)	102.038(6)	94.463(4)	98.332(4)
γ , deg	108.872(3)	90	109.365(5)	90	91.026(4)
<i>V</i> , Å ³	1990.1(6)	4467.1(14)	2310.2(12)	7711(3)	4230.8(18)
<i>Z</i>	2	4	2	8	4
<i>D</i> _{calcd} , g cm ⁻³	1.246	1.237	1.237	1.229	1.221
abs coeff, mm ⁻¹	1.456	1.627	1.802	2.203	2.476
crystal dims, mm	0.12 × 0.08 × 0.08	0.12 × 0.08 × 0.04	0.18 × 0.14 × 0.08	0.18 × 0.12 × 0.06	0.14 × 0.08 × 0.06
θ range, deg	1.39, 25.00	1.49, 25.00	1.40, 25.00	1.51, 25.00	1.18, 27.51
<i>T</i> , K	173(2)	173(2)	173(2)	173(2)	173(2)
no. of data collected	10 356	22 381	11 544	17 730	24 810
no. of obsd rfltns, <i>I</i> > 2 σ (<i>I</i>)	6868	7783	7834	6587	17 997
no. of params refined	422	475	487	379	842
GOF	1.157	1.599	1.170	1.309	1.380
R1	0.0223	0.0664	0.0382	0.0557	0.0639
wR2	0.0593	0.1265	0.1011	0.1457	0.1413

^a Graphite-monochromated Mo *K* α radiation, $\lambda = 0.710\ 73\ \text{\AA}$. R1 = $\sum||F_o| - |F_c||/\sum|F_o|$; wR2 = $[\sum(w(F_o^2 - F_c^2)^2)/\sum(w(F_o^2)^2)]^{1/2}$.

Table 4. Crystallographic Data^a for 9 and 10

	9	10
formula	C ₃₉ H ₈₉ B ₁₂ -DyNa ₃ Si ₆	C ₃₉ H ₈₉ B ₁₂ -ErNa ₃ Si ₆
fw	1087.83	1092.59
cryst syst	monoclinic	monoclinic
space group	<i>P</i> ₂ / <i>n</i>	<i>P</i> ₂ / <i>n</i>
<i>a</i> , Å	11.980(3)	11.978(3)
<i>b</i> , Å	19.160(5)	19.115(4)
<i>c</i> , Å	26.411(7)	26.350(6)
β , deg	91.890(5)	92.035(4)
<i>V</i> , Å ³	6059(3)	6029(2)
<i>Z</i>	4	4
<i>D</i> _{calcd} , g cm ⁻³	1.193	1.204
abs coeff, mm ⁻¹	1.399	1.559
crystal dims, mm	0.18 × 0.14 × 0.06	0.20 × 0.10 × 0.04
2 θ range, deg	2.62–50	3.68–50
<i>T</i> , K	173(2)	173(2)
decay, %	0	0
no. of data collected	29 042	28 891
no. of obsd rflns, <i>I</i> > 2 σ (<i>I</i>)	10 539	10 367
no. of params refined	639	639
GOF	1.490	1.561
R1	0.0596	0.0770
wR2	0.1225	0.1594

^a Graphite-monochromated Mo *K* α radiation, $\lambda = 0.710\ 73\ \text{\AA}$. R1 = $\sum||F_o| - |F_c||/\sum|F_o|$; wR2 = $[\sum(w(F_o^2 - F_c^2)^2)/\sum(w(F_o^2)^2)]^{1/2}$.

respectively. The detailed crystallographic parameters on all compounds can be found in the Supporting Information.

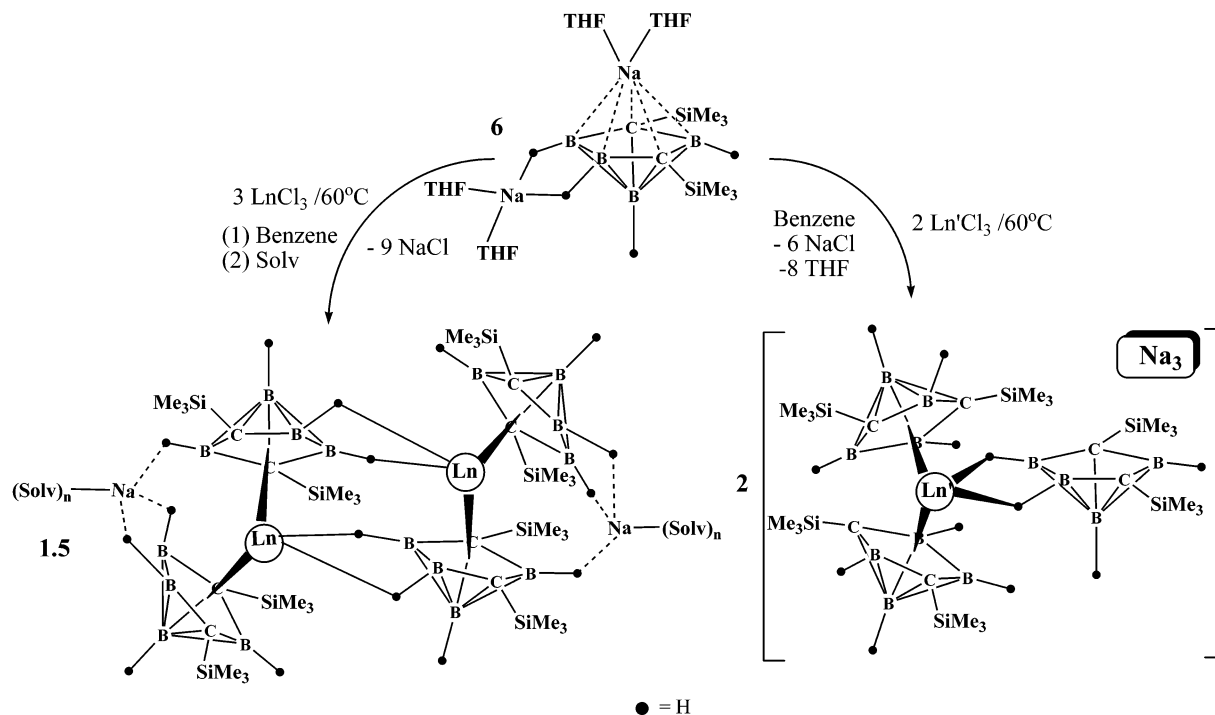
Results and Discussion

Synthesis. The reactions of *closo-exo*-5,6-Na(THF)₂-1-Na(THF)₂-2,4-(SiMe₃)₂-2,4-C₂B₄H₄ (**1**) with anhydrous LnCl₃ (Ln = Nd, Gd, Dy, Ho, Er, Tb, Lu) in molar ratios of 2:1 in dry benzene at 60 °C instead of 25 °C produced the full-sandwich lanthanacarborane complexes 2,2',4,4'-(SiMe₃)₄-3,5',6'-[(μ -H)₃Na(X)_{*n*}(Y)_{*m*}]-1,1'-*commo*-Ln(η ⁵-2,4-C₂B₄H₄)₂ (**2**, Ln = Nd, X = THF, *n* = 2, Y = none; **3**, Ln = Gd, X = THF, *n* = 3, Y = none; **4**, Ln = Dy, X = THF, *n* = 1, Y = TMEDA, *m* = 1; **5**, Ln = Ho, X = DME, *n* = 1, Y = none; **6**, Ln = Er, X = THF, *n* = 1, Y = none; **7**, Ln = Tb, X, Y = none; **8**, Ln = Lu, X = THF, *n* = 2, Y = none) in 88, 86, 70, 88, 76, 93, and 88% yields, respectively. A general synthetic procedure is outlined

in Scheme 1. These results differ markedly from those obtained in the “carbons adjacent” system, where a procedure, very similar to that used in the preparation of **2–8**, gave exclusively the trinuclear clusters of the half-sandwich lanthanacarboranes and lithiacarboranes.^{4a–d,g,k} These clusters were obtained from the room-temperature reactions of LnCl₃ with *closo-exo*-5,6-Li(THF)₂-1-Li(THF)₂-2,3-(SiMe₃)₂-2,3-C₂B₄H₄.^{4g} It is difficult to see how either the lithium cation or lower reaction temperature would favor the half-sandwich clusters. However, the “carbons adjacent” carborane requires the use of *t*-BuLi as a deprotonating agent. Since both *t*-BuLi and lanthanide compounds are known to degrade THF and other oxygen-containing compounds,^{12,13} it can be argued that such degradation reactions produce the methoxide and oxide products that effectively prevented the formation of the expected full-sandwich compounds.^{4g} The results described in Scheme 1, in which the full-sandwich complexes (**2–10**) were formed under similar conditions but in the absence of *t*-BuLi, further supports this contention. This is consistent with the fact that when the TMEDA-solvated lithiacarborane *closo-exo*-5,6-[(μ -H)₂Li(TMEDA)-1-Li(TMEDA)-2,3-(SiMe₃)₂-2,3-C₂B₄H₄] was reacted with LnCl₃, only the full-sandwich complexes were formed.^{4h} On the other hand, the reaction of the larger *nido*-C₂B₉ carborane anion with LnCl₃ in a 2:1 molar ratio produced only the expected full-sandwich lanthanacarboranes.^{1,2,14}

The effect of the reaction stoichiometry on the nature of the products was probed by studying the reactions of *closo-exo*-5,6-Na(THF)₂-1-Na(THF)₂-2,4-(SiMe₃)₂-2,4-C₂B₄H₄ (**1**) with anhydrous LnCl₃ (Ln = Dy, Er), in molar ratios of 3:1, under the same experimental conditions as those used in the preparation of **2–8**. The products were the novel mixed metallacarborane com-

- (12) (a) Jung, M. E.; Blum, R. B. *Tetrahedron Lett.* **1977**, 3791. (b) Kamata, K.; Terashima, M. *Heterocycles* **1980**, *14*, 205. (c) Schumann, H.; Palamidis, E.; Loebel, J. *J. Organomet. Chem.* **1990**, *384*, C49–52. (13) Evans, W. J.; Grate, J. W.; Bloom, I.; Hunter, W. E.; Atwood, J. L. *J. Am. Chem. Soc.* **1985**, *107*, 405–409. (14) Manning, M. J.; Knobler, C. B.; Khattar, R.; Hawthorne, M. F. *Inorg. Chem.* **1991**, *30*, 2009.

Scheme 1. Syntheses of "Carbons-Apart" Lanthanacarborane Complexes^a

^a Legend: Ln = Nd, Gd, Tb, Dy, Ho, Er, Lu; Ln' = Dy, Er; Solv = THF and/or TMEDA; $n = 1-3$.

plexes $[\text{Na}_3][1,1'\text{-}\{5,6\text{-}(\mu\text{-H})_2\text{-nido-2,4-(SiMe}_3)_2\text{-2,4-C}_2\text{B}_4\text{H}_4\}\text{-2,2',4,4'\text{-}(\text{SiMe}_3)_4\text{-1,1'-}commo\text{-Ln-(2,4-C}_2\text{B}_4\text{H}_4)_2]$ (**9**, Ln = Dy; **10**, Ln = Er), obtained as yellow crystalline solids in 78 and 82% yields, respectively (see Scheme 1). In these compounds three "carbons apart" carborane ligands were found to be associated with each lanthanide metal center, two through η^5 -bonding modes and one through a set of two Ln–H–B bonding interactions. Although these are stoichiometric analogues of tris(cyclopentadienyl)lanthanide complexes, their structures and bonding modes are quite different.¹⁵ In the lanthanocenes, all three Cp ligands are η^5 bonded to the lanthanide, giving a neutral, trigonal-planar $(\text{Cp})_3\text{Ln}$ geometry,¹⁵ while in **9** and **10** only two of the three carborane ligands are η^5 bonded. It may be that, even in the presence of the three Na^+ counterions, the high total negative charge due to the three carborane ligands (6^-) prevents a (tris) η^5 -bonding interaction. Steric considerations may also be important in such cases. However, a number of sterically crowded $(\text{C}_5\text{Me}_4\text{R})_3\text{La}$ ($\text{R} = \text{Me, Et, }^i\text{Pr, SiMe}_3$) complexes have been synthesized and structurally characterized;¹⁶ thus, it is difficult to assess the relative importance of the size of the carborane ligands in destabilizing tris complexes.

Crystal Structures. The structures of compounds **2–5** and **8** are shown in Figures 1–5, respectively, while that of **9** is given in Figure 6. Table 5 is a list of some important bond distances, and Table 6 gives some selected bond angles. All structures show that each Ln(III) ion is associated with three carborane units, two of which are η^5 bonded and the third of which is bonded through a set of two Ln–H–B bonds (see Figure 6). In

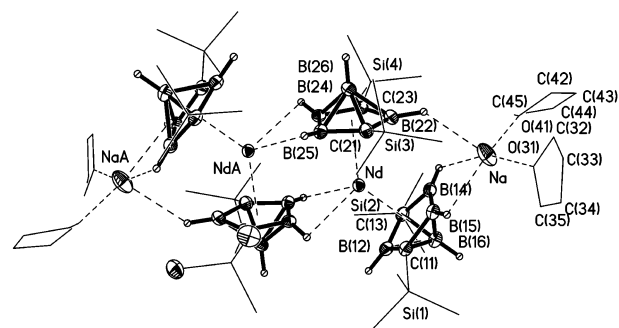


Figure 1. Perspective view of the neodymacarborane **2**. Thermal ellipsoids are drawn at the 50% probability level. The solvated THF molecules and the exo-polyhedral SiMe_3 groups are drawn with thin lines.

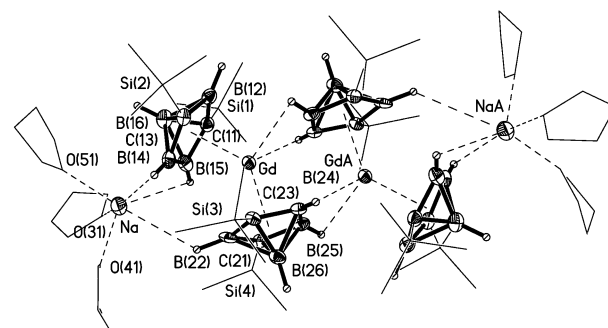


Figure 2. Perspective view of the gadolinacarborane **3**. Thermal ellipsoids are drawn at the 30% probability level. The solvated THF molecules and the exo-polyhedral SiMe_3 groups are drawn with thin lines.

the cases of compounds **2–5** and **8** these interactions led to the formation of full-sandwich metallacarborane dimers (see Figures 1–5). Each sandwich compound is also associated with a solvated Na^+ counterion. Because of the different solvent mixtures used in the isolation

(15) (a) Evans, W. J.; Davis, B. L. *Chem. Rev.* **2002**, *102*, 2119–2136. (b) Evans, W. J.; Seibel, C. A.; Ziller, J. W. *J. Am. Chem. Soc.* **1998**, *120*, 6745–6752.

(16) Evans, W. J.; Davis, B. L.; Ziller, J. W. *Inorg. Chem.* **2001**, *40*, 6341–6348.

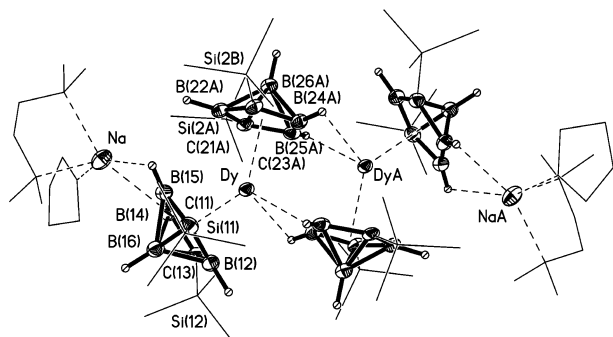


Figure 3. Perspective view of the dysprosacarborane **4**. Thermal ellipsoids are drawn at the 50% probability level. The solvated THF and TMEDA molecules and the exo-polyhedral SiMe₃ groups are drawn with thin lines.

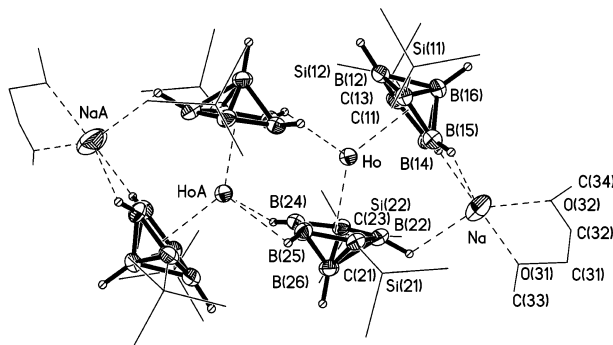


Figure 4. Perspective view of the holmacarborane **5**. Thermal ellipsoids are drawn at the 50% probability level. The solvated DME molecules and the exo-polyhedral SiMe₃ groups are drawn with thin lines.

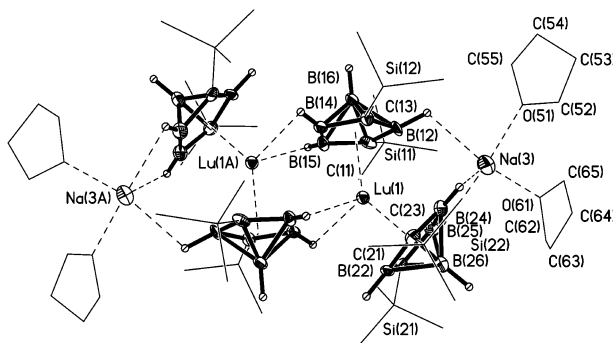


Figure 5. Perspective view of the lutetacarborane **8**. Thermal ellipsoids are drawn at the 50% probability level. The solvated THF molecules and the exo-polyhedral SiMe₃ groups are drawn with thin lines.

and purification of the compounds, different kinds and numbers of solvent molecules were found to coordinate the Na⁺ ions. For example, each Na in compounds **2** and **8** is coordinated to two THF molecules, three such molecules in compound **3**, and one THF and a TMEDA in **4**, while in **5** the solvating molecule is DME. However, the solvation environments of the Na⁺ ions seem to have little effect on the geometry of the metallacarborane complex. The bent-sandwich geometries are a common structural feature of the *commo*-lanthanacarboranes.^{1,2,4,14,17} Such geometries are also prevalent in the full-sandwich lanthanocenes,¹⁸ as well as the early

(17) Khattar, R.; Knobler, C. B.; Johnson, S. E.; Hawthorne, M. F. *Inorg. Chem.* **1991**, *30*, 1970.

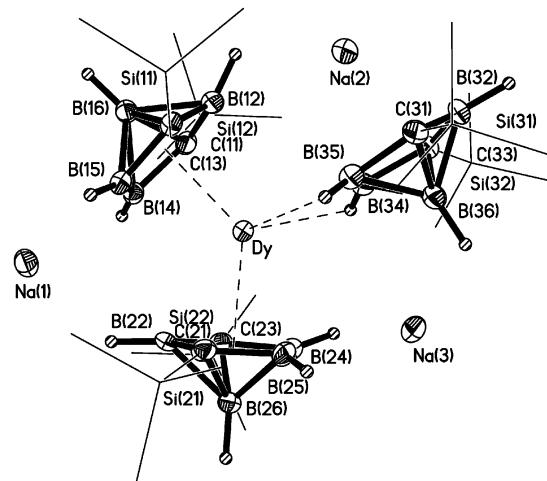


Figure 6. Perspective view of the dysprosacarborane **9**. Thermal ellipsoids are drawn at the 50% probability level. The exo-polyhedral SiMe₃ groups are drawn with thin lines. The cocrystallized hexane and benzene molecules are omitted for clarity.

d-group metallocenes of the type Cp₂MX₂.¹⁹ The Cnt(1)–Ln–Cnt(2) angles (Cnt = centroid of the particular C₂B₃ face) for the full-sandwich dimers **2**–**5** and **8** range from 134.7° for **2** to 138.2° for **8**, with an average of 136.8°, which is close to the value of 137° reported for the [U(Cl)₂(η⁵-C₂B₉H₁₁)₂]²⁻ complex¹ and that of 135.5° found for the dimeric mixed-sandwich complex {[Li(TMEDA)₂]₂{*commo*-1-[2,3-(SiMe₃)₂-2,3-C₂B₄H₄]-1-Er-[2,4-(SiMe₃)₂-2,4-C₂B₄H₄]}₂.^{4e} On the other hand, these angles are slightly larger than the average value of 128.6 ± 0.6° found in “carbons-adjacent” Ln(C₂B₄)₂ (Ln = Sm, Gd, Dy, Ho, Er) sandwich complexes^{4h} and the value of 131.9° reported for {Sm(THF)₂[η⁵-C₂B₉H₁₁]₂}⁻.² The average Ln–Cnt distances decrease in the order **2** (Nd; 2.421 ± 0.014 Å) > **3** (Gd; 2.395 ± 0.055 Å) > **4** (Dy; 2.311 ± 0.012 Å) > **5** (Ho; 2.298 ± 0.009 Å) > **8** (Lu; 2.246 ± 0.016 Å), which is the same as the decrease in the metal’s “ionic radius”, suggesting essentially electrostatic metal–carborane interactions. This same trend has been noted in the corresponding trinuclear Ln–carborane complexes^{4a–d,g,k} and in the lanthanocenes.¹⁸

The X-ray structures of **9** and **10** show that both the complexes are isostructural, with the presence of two molecules of the particular lanthanacarborane, each associated with one *n*-hexane and 1.5 benzene molecules of crystallization in the unit cell. Therefore, only the view of **9** (Figure 6) need be shown; the structure of compound **10** can be seen in our preliminary communication.^{7b} It is of interest to compare the structures of the two dysprosacarboranes **4** and **9**. An inspection of Figures 3 and 6 along with reference to the data in Tables 5 and 6 show that the environments around the Dy atoms in the two complexes are quite similar. The Dy–Cnt bond distances in **4** are 2.299 and 2.322 Å,

(18) (a) Schumann, H.; Genthe, W.; Bruncks, N. *Angew. Chem.* **1981**, *93*, 126; *Angew. Chem., Int. Ed. Engl.* **1981**, *20*, 119. (b) Schumann, H.; Genthe, W.; Bruncks, N.; Pickardt, J. *Organometallics* **1982**, *1*, 1194. (c) Maginn, R. W.; Manastyrskij, S.; Dudeck, M. *J. Am. Chem. Soc.* **1963**, *85*, 672. (d) Evans, W. J.; Wayda, A. L.; Hunter, W. E.; Atwood, J. L. *Chem. Commun.* **1981**, 292–293.

(19) Prout, K.; Cameron, T. S.; Forster, R. A.; Critchley, S. R.; Denton, B.; Rees, G. V. *Acta Crystallogr., Sect. B* **1974**, *30*, 2290.

Table 5. Selected Bond Lengths (Å) for 2–5 and 8–10

Compound 2 ^a							
Nd–C(23)#1	2.732(2)	Nd–C(21)	2.807(2)	Na–B(14)	2.717(3)	C(11)–B(15)	1.571(4)
Nd–C(13)	2.734(2)	Nd–B(25)#1	2.837(3)	Na–B(15)	2.721(3)	C(11)–B(16)	1.716(3)
Nd–B(22)	2.745(3)	Na–O(41)	2.302(2)	Si(1)–C(11)	1.857(2)	B(12)–C(13)	1.565(4)
Nd–B(14)	2.750(3)	Na–O(31)	2.333(2)	Si(2)–C(13)	1.852(2)	B(12)–B(16)	1.780(4)
Nd–B(12)	2.763(3)	Nd–C(11)	2.778(2)	Si(3)–C(21)	1.863(2)	C(13)–B(14)	1.583(3)
Nd–B(25)	2.772(3)	Nd–B(24)#1	2.779(3)	Si(4)–C(23)	1.855(2)	Nd–Cnt(1)	2.407
Nd–B(15)	2.778(3)	Nd–B(24)	2.794(3)	C(11)–B(12)	1.568(4)	Nd–Cnt(2)	2.435
Compound 3 ^b							
Gd–B(15)	2.694(8)	Si(2)–C(13)	1.857(7)	Si(4)–C(21)	1.860(7)	Na–O(31)	2.297(7)
Gd–B(12)	2.696(8)	Gd–C(11)	2.715(7)	Na–O(41)	2.296(7)	B(14)–Na#3	2.771(8)
Gd–C(23)	2.701(7)	Gd–B(25)	2.745(8)	Na–O(31)	2.297(7)	B(15)–Na#3	2.738(9)
Gd–B(24)#1	2.701(8)	Gd–B(24)	2.747(8)	Na–O(51)	2.304(7)	B(24)–Gd#1	2.701(8)
Gd–C(21)	2.702(7)	Si(1)–C(11)	1.859(7)	Na–B(15)#2	2.738(9)	B(24)–Gd#1	2.701(8)
Gd–B(22)	2.704(8)	Si(3)–C(23)	1.857(7)	Na–B(14)#2	2.771(8)	B(24)–Gd#1	2.701(8)
Gd–B(14)	2.705(8)	Si(4)–C(21)	1.860(7)	C(11)–B(12)	1.565(10)	Gd–Cnt(1)	2.340
Gd–C(13)	2.710(7)	Si(3)–C(23)	1.857(7)	Na–O(41)	2.296(7)	Gd–Cnt(2)	2.360
Gd–B(25)#1	2.713(8)						
Compound 4 ^c							
Dy–C(11)	2.659(4)	Dy–C(13)	2.681(4)	Na–N(31)	2.508(5)	C(21)–Dy#1	2.668(4)
Dy–(15)	2.664(5)	Dy–C(23)#1	2.686(4)	Na–B(14)	2.744(5)	B(22)–Dy#1	2.666(5)
Dy–B(22)#1	2.666(5)	Dy–B(24)	2.692(5)	Na–B(15)	2.751(5)	C(23)–Dy#1	2.686(4)
Dy–B(14)	2.667(5)	Dy–B(25)#1	2.701(5)	Si(11)–C(11)	1.855(4)	B(24)–Dy#1	2.705(5)
Dy–C(21)#1	2.668(4)	Dy–B(24)#1	2.705(5)	Si(12)–C(13)	1.854(4)	B(25)–Dy#1	2.701(5)
Dy–B(12)	2.671(5)	Na–O(41)	2.365(4)	Si(21)–C(21)	1.860(4)	Dy–Cnt(1)	2.299
Dy–B(25)	2.672(5)	Na–N(32)	2.443(4)	Si(22)–C(23)	1.862(4)	Dy–Cnt(2)	2.322
Compound 5 ^d							
Ho–B(15)	2.622(11)	Ho–C(21)	2.677(8)	Na–O(31)	2.188(14)	B(25)–Ho#1	2.654(9)
Ho–C(11)	2.638(8)	Ho–B(24)	2.683(9)	Na–O(32)	2.305(17)	Ho–B(15)	2.622(11)
Ho–C(23)	2.643(8)	Ho–B(14)	2.691(10)	Na–B(15)	2.639(13)	Ho–C(11)	2.638(8)
Ho–B(22)	2.644(10)	Ho–B(25)	2.707(10)	Na–B(14)	2.673(12)	Ho–C(23)	2.643(8)
Ho–B(25)#1	2.654(9)	Si(11)–C(11)	1.870(9)	Na–C(32)	2.99(3)	Ho–B(22)	2.644(10)
Ho–C(13)	2.663(8)	Si(12)–C(13)	1.860(9)	Na–C(31)	3.077(19)	Ho–B(25)#1	2.654(9)
Ho–B(24)#1	2.666(9)	Si(21)–C(21)	1.876(9)	Na–B(22)	3.124(12)	Ho–Cnt(1)	2.289
Ho–B(12)	2.666(10)	Si(22)–C(23)	1.868(9)	B(24)–Ho#1	2.666(9)	Ho–Cnt(2)	2.307
Compound 8 ^e							
Lu(1)–C(13)	2.582(7)	Lu(1)–B(15)	2.680(7)	Lu(2)–B(32)	2.635(8)	Na(3)–B(24)	2.671(10)
Lu(1)–C(21)	2.586(6)	Lu(2)–C(31)	2.598(7)	Lu(2)–B(45)	2.651(7)	Na(3)–B(25)	2.740(9)
Lu(1)–B(25)	2.590(9)	Lu(2)–B(35)	2.600(8)	Lu(2)–B(44)	2.657(8)	Na(3)–B(12)	3.172(9)
Lu(1)–B(15)#1	2.611(7)	Lu(2)–B(34)	2.606(8)	Na(2)–O(81)	2.261(8)	B(14)–Lu(1)#1	2.620(7)
Lu(1)–B(12)	2.612(7)	Lu(2)–C(41)	2.608(7)	Na(2)–O(71)	2.283(8)	B(15)–Lu(1)#1	.611(7)
Lu(1)–B(24)	2.617(8)	Lu(2)–B(42)	2.614(8)	Na(2)–B(34)	2.640(10)	B(44)–Lu(2)#2	2.621(7)
Lu(1)–B(22)	2.618(7)	Lu(2)–C(33)	2.620(7)	Na(2)–B(35)	2.697(10)	B(45)–Lu(2)#2	2.632(7)
Lu(1)–B(14)#1	2.620(7)	Lu(2)–C(43)	2.622(7)	Na(2)–B(42)	3.159(9)	Na(3)–B(12)	3.172(9)
Lu(1)–C(23)	2.626(7)	Lu(2)–B(44)#2	2.621(7)	Na(3)–O(61)	2.238(9)	Lu–Cnt(1)	2.261
Lu(1)–C(11)	2.644(7)	Lu(2)–B(45)#2	2.632(7)	Na(3)–O(51)	2.296(8)	Lu–Cnt(2)	2.230
Lu(1)–B(14)	2.654(7)						
Compound 9 ^f							
Dy–B(34)	2.650(7)	Dy–C(21)	2.727(6)	Na(1)–Na(1)#1	3.902(5)	Na(3)–B(36)	2.684(8)
Dy–B(15)	2.654(7)	Dy–C(3)	2.741(6)	Na(2)–B(32)	2.604(8)	Na(3)–B(25)	2.716(8)
Dy–B(35)	2.665(7)	Si(11)–C(11)	1.857(6)	Na(2)–C(31)	2.650(7)	Na(3)B(24)#2	2.834(7)
Dy–C(11)	2.669(6)	Si(12)–C(13)	1.870(6)	Na(2)–C(33)	2.694(7)	Na(3)–B(26)#2	2.866(7)
Dy–C(23)	2.673(6)	Si(21)–C(21)	1.875(6)	Na(2)–B(35)	2.731(7)	Na(3)–B(34)	3.172(8)
Dy–B(24)	2.686(7)	Si(22)–C(23)	1.846(6)	Na(2)–B(34)	2.743(8)	Na(3)–Na(3)#2	3.604(6)
Dy–B(14)	2.698(7)	Si(31)–C(31)	1.859(7)	Na(2)–B(12)	2.916(8)	B(24)–Na(3)#2	2.834(7)
Dy–B(22)	2.719(6)	Si(32)–C(33)	1.858(7)	Na(2) C(46)	2.938(10)	B(26)–Na(3)#2	2.866(7)
Dy–B(12)	2.721(7)	Na(1)–B(14)	2.685(7)	Na(2)–C(45)	2.978(10)	Dy–Cnt(1)	2.336
Dy–B(25)	2.723(7)	Na(1)–B(15)	2.695(7)	Na(2)–C(41)	3.048(10)	Dy–Cnt(2)	2.342
Compound 10 ^g							
Er–B(34)	2.608(10)	Er–C(21)	2.706(8)	Na(1)Na(1)#1	3.893(7)	Na(3)B(24)#2	2.832(10)
Er–B(15)	2.620(9)	Er–C(13)	2.708(8)	Na(2)–B(32)	2.594(11)	Na(3)–B(26)#2	2.860(10)
Er–B(35)	2.632(10)	Si(11)–C(11)	1.859(9)	Na(2)–C(31)	2.644(10)	Na(3)–Na(3)#2	3.597(8)
Er–C(11)	2.642(8)	Si(12)–C(13)	1.874(8)	Na(2)–C(33)	2.693(9)	B(24)–Na(3)#2	2.832(10)
Er–C(23)	2.650(8)	Si(21)–C(21)	1.876(8)	Na(2)–B(35)	2.724(10)	B(26)–Na(3)#2	2.860(10)
Er–B(24)	2.668(9)	Si(22)–C(23)	1.847(9)	Na(2)–B(34)	2.753(10)	C(62)–Na(1)#1	2.499(7)
Er–B(14)	2.673(9)	Si(31)–C(31)	1.862(9)	Na(2)–B(12)	2.897(10)	C(65)–Na(1)#1	2.326(8)
Er–B(25)	2.696(9)	Si(32)–C(33)	1.852(9)	Na(3)–B(36)	2.675(10)	Er–Cnt(1)	2.324
Er–B(22)	2.703(8)	Na(1)–B(14)	2.677(10)	Na(3)–B(25)	2.713(10)	Er–Cnt(2)	2.305
Er–B(12)	2.704(9)	Na(1)–B(15)	2.691(10)				

^a Symmetry transformation: (#1) $-x + 1, -y + 1, -z + 1$. ^b Symmetry transformations: (#1) $-x + 1, -y, -z + 1$; (#2) $-x + 3/2, y - 1/2, -z + 1/2$; (#3) $-x + 3/2, y + 1/2, -z + 1/2$. ^c Symmetry transformations: (#1) $-x + 1, -y + 1, -z + 1$; (#2) $-x - 1, -y, -z$. ^d Symmetry transformation: (#1) $-x + 3/2, -y + 1/2, -z$. ^e Symmetry transformations: (#1) $-x + 2, -y + 1, -z$; (#2) $-x + 1, -y, -z + 1$. ^f Symmetry transformations: (#1) $-x, -y + 1, -z + 1$; (#2) $-x, -y, -z + 1$; (#3) $-x + 1, -y + 1, -z + 1$. ^g Symmetry transformations: (#1) $-x, -y + 1, -z + 1$; (#2) $-x, -y, -z + 1$; (#3) $-x + 1, -y + 1, -z + 1$.

Table 6. Selected Bond Angles (deg) for Compounds 2–5 and 8–10^a

Compound 2					
B(16)–C(11)–Nd	100.31(13)	B(24)#1–C(23)–Nd#1	75.72(12)	B(24)#1–C(23)B(22)#1	112.23(19)
B(16)–B(14)–Nd	99.83(14)	C(23)#1–B(24)–B(25)#1	105.02(19)	C(21)–B(22)–C(23)#1	105.2(2)
B(16)–B(12)–Nd	99.16(14)	B(26)–B(22)–Nd	101.40(14)	B(26)–B(24)–Nd	99.71(14)
B(12)–C(13)–B(14)	112.4(2)	Nd–B(25)–Nd#1	93.24(8)	C(21)#1–B(25)–B(24)#1	105.36(19)
B(16)–C(13)–Nd	102.38(14)	B(16)–B(15)–Nd	98.63(14)	B(26)#1–B(25)–Nd#1	97.98(14)
B(26)–C(21)–Nd	100.69(13)	B(22)–C(21)–B(25)#1	112.1(2)	Cnt(1)–Ln–Cnt(2)	134.7
Compound 3					
B(12)–C(11)–B(15)	111.8(6)	B(16)–C(13)–Gd	99.5(4)	B(26)–B(25)–Gd#1	126.4(5)
B(16)–C(11)–Gd	100.0(4)	B(16)–B(15)–Gd	98.9(4)	B(26)–B(24)–Gd#1	126.3(4)
B(16)–B(14)–Gd	97.8(4)	B(25)–C(21)–B(22)	112.7(6)	B(26)–B(24)–Gd	97.9(4)
B(16)–B(12)–Gd	98.1(5)	B(26)–C(21)–Gd	101.5(4)	Cnt(1)–Ln–Cnt(2)	137.2
B(26)–C(23)–Gd	101.3(4)	B(26)–B(22)–Gd	99.2(4)		
Compound 4					
B(16)–B(12)–Dy	98.1(3)	B(26)–C(21)–Dy#1	101.5(2)	Dy–B(24)–Dy#1	92.70(14)
B(16)–C(11)–Dy	100.2(2)	B(26)–B(22)–Dy#1	99.6(2)	Dy–B(25)–Dy#1	93.23(14)
B(16)–B(14)–Dy	98.4(2)	B(26)–C(23)–Dy#1	100.9(2)	Cnt(1)–Ln–Cnt(2)	136.9
B(16)–B(15)–Dy	35.42(14)	B(26)–B(24)–Dy	125.5(3)		
Compound 5					
B(16)–C(13)–Ho	99.0(5)	B(26)–C(21)–Ho	100.1(5)	B(26)–C(23)–Ho	101.9(5)
B(16)–B(14)–Ho	97.2(5)	B(16)–B(12)–Ho	97.4(5)	B(26)–B(25)–Ho	97.5(5)
B(26)–B(22)–Ho	99.5(5)	B(16)–C(11)–Ho	100.7(5)	Cnt(1)–Ln–Cnt(2)	137.1
Compound 8					
B(16)–B(14)–Lu(1)	97.8(4)	B(26)–C(21)–Lu(1)	100.5(4)	B(26)–B(25)–Lu(1)	104.7(6)
B(26)–B(22)–Lu(1)	97.0(4)	B(16)–B(15)–Lu(1)#1	125.3(5)	B(26)–B(24)–Lu(1)	96.9(4)
B(16)–C(11)–Lu(1)	99.5(4)	B(16)–B(15)–Lu(1)	96.5(4)	B(16)–B(12)–Lu(1)	99.3(4)
B(16)–C(13)–Lu(1)	102.0(4)	B(26)–C(23)–Lu(1)	98.0(4)	Cnt(1)–Ln–Cnt(2)	138.2
Lu(1)#1–B(14)–Lu(1)	93.8(2)				
Compound 9					
B(26)–C(21)–Dy	99.9(3)	B(16)–C(13)–Dy	99.1(3)	Dy–B(15)–Na(1)	113.7(3)
B(16)–C(11)–Dy	101.5(4)	B(26)–B(22)–Dy	98.5(4)	Dy–B(35)–Na(2)	100.4(2)
B(16)–B(14)–Dy	98.6(4)	B(26)–B(25)–Dy	98.3(4)	Cnt(1)–Ln–Cnt(2)	131.0
B(16)–B(12)–Dy	98.3(4)	B(26)–C(23)–Dy	101.9(3)		
Compound 10					
B(16)–B(15)–Er	100.9(5)	B(26)–C(21)–Er	99.6(5)	B(36)–C(31)–Na(2)	102.6(5)
B(16)–C(11)–Er	101.3(5)	B(16)–B(14)–Er	98.5(5)	B(36)–C(33)–Na(2)	100.5(5)
B(26)–B(25)–Er	98.0(5)	B(26)–B(22)–Er	97.8(5)	Er–B(12)–Na(2)	95.1(3)
B(16)–B(12)–Er	97.5(5)	B(26)–C(23)–Er	101.8(5)	Er–B(15)–Na(1)	114.6(3)
B(16)–C(13)–Er	99.0(5)	B(36)–B(34)–Er	122.8(6)	Cnt(1)–Ln–Cnt(2)	130.9

^a See Table 5 for definitions of the symmetry transformations.

which are slightly smaller than the equivalent distances of 2.336 and 2.342 Å in **9**, while the Cnt–Dy–Cnt bond angle in **4** is larger than that found in **9** (136.9° compared to 131.0°). The Dy–B(34,35) distance in **9** is 2.657 ± 0.007 Å, compared to 2.703 ± 0.002 Å for the equivalent distances in **4**, indicating a closer approach of the bridging carborane in **9**. The closer approach of the η²-bonded carborane and the larger bond angle and bond distances in **9** are all internally consistent, but there is no way of assessing which of these is the dominant interaction and which are consequences.

In all cases each lanthanide metal atom is associated with three carboranes, two of which are η⁵ bonded and the other being η² bonded. When excess carborane ligand is present, it is incorporated as the η²-bonding group; otherwise, dimeric compounds, such as **2–8**, are formed.

IR and NMR Spectroscopy. All compounds were also characterized by IR spectroscopy and elemental analyses. Except for the fact that the analytical samples contain no hexane in **9** and one additional THF molecule of solvation in **8**, the results of these analyses are consistent with the crystal structures. The IR spectra of the lanthanacarboranes all exhibit well-resolved multiple terminal B–H stretching vibrations in the 2270–2590 cm⁻¹ range. Such fine structures of B–H stretching bands have been previously observed in other

closo- and *commo*-lanthanacarboranes and lithiacarborane. They have been explained on the basis of unequal interactions of the boron-bound hydrogens with metal groups present in the complex.^{4g,h,j} Because of the strong paramagnetism of complexes **2–7**, **9** and **10**, no useful NMR spectra could be obtained. However, the diamagnetic lutetium complex **8** was found to provide interpretable NMR data. The ¹H NMR spectrum of **8** showed two broad singlets at δ 3.71 and 1.56 ppm due to the CH₂ groups of THF and two singlets at δ 0.74 and 0.68 ppm which were assigned to the CH₃ protons of the SiMe₃ groups. The ¹³C NMR spectrum showed the presence of the cage carbons and THF molecules, plus two quartets due to the CH₃ carbon atoms of the SiMe₃ groups at δ 2.19 and 1.84 ppm, respectively. The resonance doublets for the SiMe₃ hydrogens and carbons indicate two different chemical environments for the trimethylsilyl groups. Reference to Figure 5 shows two different sets of carborane groups in compound **8**, which could account for the multiple resonances. The ¹¹B NMR spectra show broad peaks at δ 28.5 and 7.0 ppm and a well-resolved doublet at δ -47.3 ppm (apical B) in a 1:2:1 ratio. While all three of these should be doublets due to the presence of the cage hydrogens, the broadness of the two downfield resonances could prevent their resolution. This 1:2:1 peak area pattern and the chemical shifts are very similar to that of the precursor *closo*-

exo-5,6-Na(THF)₂-1-Na(THF)₂-2,4-(SiMe₃)₂-2,4-C₂B₄H₄, which shows a set of three doublets at δ 16.3, 5.4, and -54.2 ppm.⁸ It has been observed that the replacement of an apical group 1 element such as sodium by p- or d-block metal groups gives rise to significant deshielding of the apical boron, B(6), resulting in a large downfield shift of its resonance from $\delta \sim -50$ ppm to the $\delta -10$ to 0 ppm range, while the basal boron resonances experience much smaller chemical shift changes. The relatively large apical boron shifts on metalation have been qualitatively explained by noting that the capping metal and the apical boron compete for electron density in the C₂B₃ bonding face and that covalent metal-carborane interactions will tend to drain electron density away from the apical boron toward the metal group, resulting in a downfield shift in its resonance.²⁰ Therefore, the small change of the chemical shift of the apical boron resonance on coordination to Lu is consistent with the predominantly ionic lanthanide-carborane interaction. It should also be pointed out that there is no definitive way of proving that the solid-state structure of compound **8**, shown in Figure 5, is a valid representation of the solution species. However, the solubility of the lanthanacarboranes in solvents such as benzene indicate that there is not extensive ionization in solution.

Magnetic Susceptibilities. The molar magnetic susceptibilities of compounds **9** and **10** followed the Curie-Weiss law, $\chi = C/(T - \Theta)$, with $\Theta \approx 0$ K, indicating only very weak magnetic interactions. The Curie constants, *C*, correspond to effective magnetic moments of 10.4 and 9.76 μ_B per atom for Dy³⁺ (**9**) and Er³⁺ (**10**) with their ⁶H_{15/2} and ⁴I_{15/2} ground states, respectively. The results indicate that crystal field effects play little or no role in the temperature range studied and that free ion behavior can be safely assumed. This was the same conclusion reached earlier for Dy and Er complexes.²¹

EPR Spectroscopy. Compounds **2**, **3**, and **5** were studied by X-band EPR spectroscopy at 4 K as polycrystalline powders or in glassy frozen solutions (THF for **3** or benzene/toluene mixtures for **2** and **5**). The diholmium complex **5** (Ho³⁺: ⁵I₈ ground state) showed no EPR response between 0.1 and 1.0 T magnetic field range. The dineodymium compound **2** (Nd³⁺: ⁴I_{9/2} ground state) exhibits line-rich EPR spectra between 0.05 and 1.0 T with considerable differences between solid and frozen-solution samples, suggesting effects of

spin-spin coupling between the two 4f³ centers. An EPR analysis of **2** must therefore rely on corresponding studies of related mononuclear compounds, which we plan to synthesize and investigate in the future.

The digadolinium compound **3** shows a single, very broad (0.2 mT) EPR signal centered at *g* = 2.030 (solid) or *g* = 2.038 (frozen THF solution). This result differs from observations of partially resolved spectra reported by us^{4h} and others.²² Because of the relatively simple configuration of Gd³⁺ (4f⁷: ⁸S_{7/2} ground state) and its relevance for MRI enhancement the EPR spectra of mononuclear and dinuclear gadolinium complexes have been tentatively analyzed in terms of zero-field splitting contributions.²² Unfortunately, the absence of spectral structuring and the broadness of the signal preclude any detection of possible intermetallic interactions, either within the molecule **3** (3.969 Å Gd-Gd distance) or between molecules (smallest intermolecular Gd-Gd distance 14.291 Å).

Conclusions

The reactions of the "carbons-apart" *closo-exo*-5,6-Na(THF)₂-1-Na(THF)₂-2,4-(SiMe₃)₂-2,4-C₂B₄H₄ (**1**) with a number of LnCl₃ salts, in molar ratios of 2:1 and 3:1, produced full-sandwich lanthanacarborane complexes in which each Ln(III) occupies the apical positions above the open faces of two carborane dianions and is bonded to a third by two Ln-H-B bridges. If excess carborane is not available, this bonding pattern is achieved by dimerization (compounds **2-5** and **8**).

Acknowledgment. This work was supported by grants from the National Science Foundation (Nos. CHE-9988045 and CHE-0241319), the donors of the Petroleum Research Fund, administered by the American Chemical Society, The Robert A. Welch Foundation (No. N-1322 to J.A.M.), and Northern Illinois University through a Presidential Research Professorship. N.S.H. gratefully acknowledges the Forschungspreis der Alexander von Humboldt-Stiftung (Bonn, Germany).

Supporting Information Available: Tables of crystallographic data, including fractional coordinates, bond lengths and angles, anisotropic displacement parameters, and hydrogen atom coordinates, for **2-5** and **8-10**; these data are also available as CIF files. This material is available free of charge via the Internet at <http://pubs.acs.org>.

OM030426X

(20) Maguire, J. A.; Ford, G. P.; Hosmane, N. S. *Inorg. Chem.* **1988**, *27*, 3354.

(21) Birmingham, J. M.; Wilkinson, G. *J. Am. Chem. Soc.* **1956**, *78*, 42-44.

(22) (a) Rizzi, A.; Baggio, R.; Calvo, R.; Garland, M. T.; Pena, O.; Pereg, M. *Inorg. Chem.* **2001**, *40*, 3623-3625. (b) Avecilla, F.; Platas-Iglesias, C.; Rodriguez-Cortinas, R.; Guillemot, G.; Bünzli, J.-C. G.; Brondino, C. D.; Geraldès, C. F. G. C.; de Blas, A.; Rodriguez-Blas, T. *Dalton* **2002**, 4658-4665.